Solvent Transport Behavior of Shear Aligned Graphene Oxide Membranes and Implications in Organic Solvent Nanofiltration

Abozar Akbari [1], Sally E. Meragawi [1], Samuel T. Martin [1], Ben Corry [2], Ezzatollah Shamsaei [3], Christopher D. Easton [4], Dibakar Bhattacharyya [5], Mainak Majumder[1]*

[1] Nanoscale Science and Engineering Laboratory (NSEL), Department of Mechanical and Aerospace Engineering, Monash University, Clayton, VIC 3800, Australia.

[2] Research School of Biology, Australian National University, Canberra, ACT, Australia.

[3] Department of Chemical Engineering, Monash University, Clayton, VIC 3800, Australia.

[4] CSIRO Materials Science and Engineering Bayview Avenue, Clayton, VIC 3168, Australia.

[5] Department of Chemical and Materials Engineering, University of Kentucky, Lexington, Kentucky, 40506, USA.

*Corresponding author E-mail: mainak.majumder@monash.edu

KEYWORDS: Graphene, Graphene oxide, membrane, Solvent transport, Organic solvent, Nanofiltration

ABSTRACT:

Solvent transport in membranes composed of stacked sheets of graphene oxide (GO) with molecular scale channels and a complex arrangement of hydrophobic and hydrophilic domain is not well-understood. Here, we observe that the interlayer space between GO sheets expands in different solvents without disturbing the membrane integrity, and is typically larger in the aqueous medium compared to the non-aqueous mediums. But, the membranes have a tighter molecule sieving feature in aqueous medium demonstrated by lower permeance and higher solute rejection arising from interfacial water layers 'sticking' to charged polar groups. As a result of this polar interaction, the permeance of polar solvents in GO membrane scales inversely to the polarity of the solvent, which is contrary to other polymeric and ceramic hydrophilic membranes, and also scales inversely to the viscosity of solvents as per continuum expectations. We highlight the extended solvent-handling space of GO membranes such as in polar protic, polar aprotic and non-polar solvents demonstrating versatility over a commercial nanofiltration membrane and predict exciting new applications in advanced separation engineering.

Introduction:

Carbon-based membranes such as those based on carbon nanotubes, graphene and graphene oxide show promise as next -generation separation membranes, due to their novel and exciting transport properties such as high selectivity and high permeance for both liquids [1, 2] and gases [3]. Mass transport through the carbon-based nanochannels has become an emerging area of research with a widespread interest in purifications , supercapacitors [4], lithium-sulfur-batteries [5], and micro-nanofluidics [6]. Amongst carbon-based membranes, those made from graphene oxide (GO), a derivative of graphite, has attracted significant attention because of the possibility of easy production of the input raw material, GO [7]. In comparison with graphitic nanochannels, where the graphene walls are stacked together by van der Waals forces, with adjacent sheets distanced at around ~3.4 Å, in GO nanochannels in the dried state, the GO sheets are held together by a combination of hydrogen bonding and van der Waals forces and the interlayer spacing of GO sheets (d) ranges between 6 Å, to 12 Å (depending on the humidity) [8, 9] , which are truly molecular scale channels capable of transporting molecules and ions [1, 9], gases [10, 11], and fluids [12]. GO membranes are decorated with different functional groups such as hydroxyl, carboxyl and epoxy groups, which make it amenable for modification to specific separation targets[13]. Several reports on permselectivity performance of GO membranes in nanofiltration applications and extreme operating environment experiments also have revealed the high robustness of GO membranes in harsh conditions [14]. Additionally, GO membranes can be easily fabricated or assembled by re-stacking the exfoliated GO sheets by vacuum filtration [15] or/and layer-by-layer assembly of the membrane through dip coating of a porous support in a GO dispersion [16], or via the alignment of nematic phase GO dispersions on a porous support, by a fluid shearing device [2, 5, 17, 18].

Many published reports in the last few years have dealt with experiments and simulations of liquid transport through graphene oxide nanochannels, typically water. GO is a unique system to examine liquid transport characteristics because of the amphiphilic nature of the substance. The GO sheets have sp^2 domains, interspersed with polar groups indicating that a wide range of interactions such as van der Waals, electrostatic, polar, hydrogen bonding will be operative [19-21]. Some of this behavior is evidenced in the surfactant-like properties of GO and good dispersability including liquid crystalline behavior in polar protic and aprotic solvents [20, 22]. While there have been a few studies reporting organic solvent transport properties of GO membranes[23-25], further investigation is needed as it is not hard to recognize the potential of GO membranes for nanofiltration in organic solvents given the chemical inertness of carbon. Further understanding of how the interactive forces in GO govern the transport and separation characteristics in different environments is needed. To probe this we have chosen a wide range of aqueous and non-aqueous mediums and marker solutes and undertaken comprehensive studies on permselectivity of the GO membrane.

Results & Discussions

GO membrane was fabricated by the shear-alignment of a nematic phase dispersion of GO (at 30 mg/mL concentration), on a Polyvinylidene Fluoride (PVDF) porous support (with a 200 nm pore size) by a method reported elsewhere [2] (Figure 1a,b and Supplementary Section 2). Scanning electron microscopy imaging (Figure 1c) has shown uniformity and continuity of the thin GO membrane with a thickness ~100 ±20 nm (Supplementary Section 3). Due to a well-ordered interconnected network of channels, shear-aligned GO membranes have shown high liquid permeance and retention for organic molecules [2, 5]. Fourier transform infrared spectroscopy (FTIR) has revealed that the interconnected nanochannels are a complex of

hydrophilic (oxidized) and hydrophobic (non-oxidized) regions (Supplementary Section 4). Since during sonication of graphite oxide, GO sheets would break from weaker parts, it is widely accepted that the hydrophilic regions are located predominantly at the sheet edges [26, 27]. The hydrophilic regions act as a spacer and define the interlayer spacing between adjacent GO sheets[28] while simultaneously regulating water permeance as electrostatic gates[29].

Permeance & Retention Properties: A dead-end filtration system (Sterlitech HP4750 High Pressure Stirred Cell) was used to characterize permselectivity of the GO membrane in aqueous and non-aqueous mediums. For understanding the difference between separation and permeances of GO membranes in aqueous and non-aqueous polar solvents, deionized water (DI water) along with ethanol and IPA which are commonly used in the pharmaceutical and chemical industries, were selected as the solvents of interest (Supplementary Section 8). A collection of organic molecules with different molecular weights (MW), including Methyl Red (MW: 269.3 Da), Rhodamine B (MW: 479.03 Da), Rose Bengal (MW: 973.67 Da), and Tannic Acid (MW: 1701.19 Da) were used to study the solute retention. It should be noted that all the organic molecules formed a homogenous and stable solution with the solvents (Supplementary Section 8). The GO membrane (~100 ±20 nm) demonstrated higher permeance for the non-aqueous solvents and the steady state permeance is largest for ethanol (180±10 LMH/bar) and lowest for water (92±12 LMH/bar) (Figure 1d and Table S2). We report the steady state permeance numbers when the variation of the flux was not more than 2% per 10 min (typically after 3 hours), for five different measurements on three different membranes. We also observe a significant drop in water permeance with time which can be attributed to water sorption and hydration of the GO membranes, as these experiments begin with a dried membrane [24]. Irrespective of the solvents, the retention of the membrane for the solutes is consistent with

molecular weight with the highest retention for Tannic acid, followed by Rose Bengal, Rhodamine B, and Methyl Red, respectively (Figure 1e). However, the retentions are consistently higher in water than in alcohols, for e.g. methyl red which can be considered an electro-neutral molecule at pH of 7, the rejection is 99%, and this declines to 61 % in IPA and 39% in ethanol suggesting a tighter sieving feature in water.

***Overview of solvent transport of GO membrane vis-à-vis other membranes*:** A large body of work on non-aqueous solvent and solute transport through polymeric membranes have shown, both experimentally and theoretically, that the separation performance in organic solvents are less predictable compared to aqueous environments [30, 31] due to different interactions such as surface tension, polarity, swelling, and hydrophobicity or hydrophilicity of the interfaces.

Slip flow theory has been the basis for understanding the anomalously fast water flow through graphitic nanochannels relying on low friction or frictionless flow/interactions between water molecules and the channel walls [32]. The case of GO membranes is different. The presence of a large proportion of oxidized groups in the graphitic nanochannel (O/C ~ 0.40 - Supplementary Section 5) will purportedly lead to high friction/interactions between water molecules and the walls of the two dimensional and labyrinthine flow channels [26, 33]. Simulation and computational investigations have shown that hydrogen bonding and van der Waals forces dominate the interactions that result in water molecules clustering in the oxidized regions [33]. The clustered water molecules have lower transport mobility and the inherent tortuosity in this structure enhance the side-pinning effect, as the water molecules traverse from one layer to the other. Such effects interrupt the ultrafast flow that occurs in the pristine graphite regions [34].

To gain an overview of GO membrane transport, we contrasted literature data on typical permeances of water & ethanol, noting that these solvents have different polarity but almost similar viscosity. For example, in some reports the larger water permeance compared to polar organics in carbon nanotubes have been attributed to the reduced interaction of water with the graphitic channels [32, 35]. In hydrophobic polymeric membranes, the polarity of the solvent has a negative effect on the permeance, i.e. the water permeance is smaller than the ethanol permeance; the opposite is true for hydrophilic membranes [36] (Figure 1f). The same behavior is also observed in the case of the hydrophilic ceramic membrane such as TiO_2 and ZrO_2 membranes, where water permeances are larger than ethanol permeances [37]. It is interesting to note that despite the overall hydrophilicity of GO membranes (water contact angle ~45°, Supplementary Section 7), an inverse scaling, contrary to expectations, is observed with solvent polarity, i.e. the water permeance is smaller than the ethanol permeance. We note that the permeances of different membranes shown in Figure 1f is for comparison between water and ethanol and have not been corrected for membrane thickness.

Therefore, here, we argue that the polarity of the solvent, represented by the dielectric constant (ε), can be used to qualitatively estimate the degree of interaction of the GO membranes with the solvents. The dielectric constant of the solvent provides a measure of the interactions between a solvent and the membrane, for e.g. the solvation layers on surfaces and around charged particles[19] , the van der Waals forces between solute particles in a solvent[19], the scaling of various interfacial electrostatic effects either by the Debye length or otherwise[19], and the ionization constant (pKa) of acidic groups increases as ε decreases.[38]

Interaction of solvents with GO membranes and implications in retention: In GO membranes, if the functional groups are considered to be attached primarily to the defective graphene sheet

edges, then the ends of the GO nanochannels are hydrophilic while the interior is approximately hydrophobic. The polar 'end-effects' gives rise to cohesive interactions with the polar solvents, while the 'channel-effects' enables low interaction flows of the solvents [26]. The GO membrane (~100 ±20 nm thick) showed higher permeance for ethanol (180±10 LMH/bar) and IPA (130±10) than water (92±12), respectively, which is attributed to their lower polarity, resulting in reduced interaction with the channel ends (hydrophilic regions of the channels). Ethanol showed a higher tendency to permeate through GO nanochannels compared to IPA, which is attributed to lower viscosity (Table S2). The permeation results are consistent with molecular dynamic simulations of water and ethanol transport through GO nanochannels conducted by Simon Gravelle et al. [39] which showed higher affinity of ethanol to permeate in GO membrane than water. Possible intermolecular interactions involved in fluid transport are van der Waals forces, specifically dipole-dipole interactions and hydrogen bonding[19, 40, 41]. For a surface with the ionized group in a highly polar solvent such as water, the strong ion-dipole interactions will orient the layers of water molecules around the ionic charge [19, 41]. When compared with ethanol and IPA, water molecules have a much higher dielectric constant (ε), which provides an appropriate environment for dissociation of the ionizable groups on the GO sheets[19, 40, 41 38, 42]. In the organic solvents pK_a of acidic groups on the GO, sheets shift to much higher values as a result, dissociation of acidic groups is much less probable. For example, carboxylic groups which could be the main source of negative charges in the GO sheets ($-COOH \rightarrow COO^- + H^+$) is able to dissociate in water but not in the organic solvent[40]. The large attractive ion-dipole forces between highly polar water molecules and the carboxylic ions affect the orientation of water molecules close to the GO sheet. We have observed significantly larger retention by the GO membrane for all the solutes in an aqueous environment, compared to the polar organic

environments (Figure 1e). It can to some extent be attributed to hydration and enlargement of the effective solute size [30, 43]. Geens and Van der Bruggen [43] combined the Stokes-Einstein and Wilke-Chang equations to find the ratio of effective solute diameters of a solute in two different solvents, using this correlation:

$$\frac{d_{s_2}}{d_{s_1}} = \left(\frac{\emptyset_{s_1} MW_{s_1}}{\emptyset_{s_2} MW_{s_2}}\right)^{0.5} \qquad (1)$$

where, d, $\emptyset$, and MW are the effective diameter of the solute, association parameter (Water: 2.6, ethanol: 1.9, IPA: 1) of the solvent, and the molecular weight of the solvent, respectively, while s_1 and s_2 distinguish between solvent 1 and solvent 2. Based on this correlation and with ~ 4.87Å and ~ 5.88Å as the hydrated radius of Methyl red and Rose Bengal [2], solvated radius of Methyl Red and Rose Bengal in IPA will be ~ 4.30Å and ~ 5.19Å, while it will be ~ 3.49Å and ~ 4.22Å in ethanol, respectively, suggesting that the smaller solvated radius could only play a minor role in decreasing the rejections.

Another reason for the lower solute retention of the GO membrane in IPA and ethanol is also due to lower electrostatic interactions between the membrane and solutes in the organic mediums, because the solutes under consideration all have charges, despite some being electro-neutral (Methyl Red and RhodamineB). Because of the low dielectric constant of the non-aqueous solvent, ionization of the acidic groups in the GO membrane, which is the main source of negative charge, in this case, is limited and these functionalities cannot contribute to the electrostatic forces to repelling or adsorbing the solutes [38, 40]. This also can be seen in the retention performance in Figure 1e where adsorption has minimal contribution to retention in the organic environments.

The enhanced interactions arising from the polarity of the solvent and the membrane that lead to a lower permeance of the GO membrane for water compared to less polar solvents may be similarly used to explain the retention behavior of the GO membrane. It is likely that a layer of interfacial water on the surface of the graphene oxide laminates is formed, resulting in a steric like exclusion of the solute and improved retention of solutes by the GO membrane.

Interlayer Spacing of Graphene Oxide sheets in solvents: A plausible reason behind the lower selectivity of the GO membrane in the non-aqueous mediums is due to the interstitial spacing of the GO sheets in the membrane structure in a particular solvent. It is noted that the molecular transport through the GO membrane is determined by both the interlayer spacing between two adjacent GO sheets and the in-plain voids of the GO sheets. Given the size of the solutes we are investigating, it can be accepted that interlayer distance has a dominant effect on our experiments [27, 44]. To investigate this, XRD was used to study the variance in the interlayer space between GO sheets when in contact with the solvents (Supplementary Section 6). Results showed that the interlayer space increases when the membrane is in contact with the solvents, with the greatest change in interlayer spacing (d) measured for membranes in water (in water ~21.2 Å, in ethanol ~11.5 Å, and in IPA ~10.8 Å) (Figure 2a). These results are counter-intuitive to the permeations and retention studies where the membranes in highly polar water medium showed lower permeance and higher retention for the organic solutes. However, the XRD analysis agrees with expectations from Derjaguin-Landau-Verwey- Overbeek (DLVO) theory. DLVO can be used to describe the energy of interaction between adjacent GO sheets in terms of both attractive van der Waals (vdW) and repulsive electrostatic (EL) interactions. The equilibrium of these competing interactions defines the driving force for changes in the interlayer spacing [38]. As water, IPA and ethanol have similar refractive indices (1.33, 1.38, and 1.36, respectively [45]), GO sheets have

similar Hamaker constants in all of the solvent [38, 46, 47]. Since Hamaker constant defines van der Waals force between two particles in the absence of influence of intervening medium between them, the van der Waals forces between GO sheets in water, ethanol and IPA would be similar. So, the interlayer space of GO is controlled effectively by the electrostatic interactions between GO sheets in the presence of medium.

As discussed earlier the ionization of the carboxylic groups in GO sheets are precluded by the low dielectric constant of IPA and ethanol and promoted by the high dielectric constant of water[38, 40]. The extent of this electrostatic interaction & the associated length scale can be described by Debye length (λ_D):

$$\lambda_D = \sqrt{\frac{\varepsilon\varepsilon_0 k_B T}{2N_A e^2 I}} \qquad (2)$$

where ε is the dielectric constant of solvent, ε_0 is the permittivity of vacuum, k_B is Boltzmann's constant, T is the absolute temperature, $N_A$is Avogadro's number, e is the elementary charge, and I is the ionic strength of solution. Although in most cases, the strength of the ionic concentration in aqueous mediums is varied to achieve changes in Debye length and strength of ionic interaction; here we varied the dielectric constant of the solvent as means to vary the strength of interaction and we found that $d \propto \varepsilon^{0.48}$ (Figure 2b). We also note that aqueous ionic strength dependent interlayer swelling has been observed by Zheng et al.[48] Based on Equation (2), and correlation between Debye length and dielectric constant ($\lambda_D \propto \sqrt{\varepsilon}$.), it is suggestive of this notion that the equilibrium distance between GO sheets is changing due to changes in the size of the repelling double layers. While this hypothesis is reductive, it does not, for instance, consider the role the dielectric constant plays in the other forces, such as the van der Waals forces or the

variability in ionic strength in the different electrolytes, it is instructive to consider this simplified model to give intuition into the system's otherwise complex behavior.

Effect of interfacial water: To investigate the effect of interfacial water on hydrodynamic pore size of GO membrane, we pre-treated a dried GO membrane (~100 ±20 nm thick) by soaking the membrane in water, and then examining permselectivity characteristics of the water pre-treated membrane in the non-aqueous solvents (Supplementary Section 8.3). Results showed that the permeance of the membrane for ethanol and IPA decreases and retention performance improved when the membrane is pre-treated with water (Figures. 3a,b). These evidences promote the idea of smaller hydrodynamic pore size of the GO membrane in water medium compared with the non-aqueous mediums, due to the orientation of water molecules in the vicinity of negatively charged parts of the GO nanochannels. These experiments reinforce the role interfacially immobilized water plays in regulating transport & selectivity in GO membranes. The immobilized water between the membrane interlayers gradually leaves the membrane as the alcoholic solvents permeate through the membrane indicating that GO membranes can permeate water-alcohol mixture, which is rather difficult for established polymeric nanofiltration membranes. We can also speculate that GO membranes can function in a manner similar to biological membrane channels through a self-regulating layer of 'water-gates' along the hydrophilic domains of the GO sheets and can be adapted to undertake separations in polar solvents [49].

Molecular Dynamics Simulations: To understand the interaction of the solvents with different functional groups, we carried out molecular dynamics simulations of pristine graphene surfaces and surfaces containing one of a variety of functional groups (more details in Supplementary Section 9). These groups include epoxy, hydroxyl, carboxyl and carboxylateand were chosen

based on the fact that they represent the functional groups believed to be present in graphene oxide [8]. As an indication of how the different surfaces might influence the transport rates of solvents, we calculate the average time solvent molecules dwell near the functional group. While this is not a direct measure of transport rates, longer dwell times in these equilibrium simulations are likely to represent slower transport rates in non-equilibrium situations as has been seen in dwell time analysis of transport in biological pores [50]. The dwell time is calculated by the amount of time a specific solvent oxygen spends close to the functional group after its initial approach (see Supplemental Section 9).

The values shown in Table1, indicate that on a pristine surface the average dwell time of water molecules is smaller than for the alcohols, suggesting faster transport of water in the graphitic domains. IPA has the longest dwell time on the pristine surface, indicative of stronger interactions with the surface and slower transport rates. It can be seen that the presence of functional groups increases the dwell times in our simulations, with the more polar groups having the largest values. As the presence of charged carboxylate groups has by far the largest influence on dwell times, one expects that the transport rates will be slowest in solvents with large dielectric constants in which these charged groups can form. For example, the presence of charged carboxylate groups results in the formation of hydrogen bonds with multiple surrounding water molecules (Figure 4a), holding them for extended periods of time close to the functional group. While a carboxyl on average forms a hydrogen bond to one ethanol molecule (Figure 4b), it does not trap as many solvent molecules for as long. Thus, as carboxylate groups can form in water but are unlikely to be found in ethanol, the transport of water is expected to be slower than for ethanol as seen in our experimental results. Also notable is that IPA has a larger

dwell time around most of the functional groups compared to ethanol, which would yield slower transport along the GO surface as also seen in our experimental data.

Scaling behaviour: To investigate the transport characteristics of different solvents, a GO membrane, with larger thickness of ~350±20 nm was fabricated on a porous Nylon substrate (Nylon 66, pore size 0.2 mm, MDI, India), by our method (Supplementary Section 2). The choice of the support membrane is dependent upon the solvents we wish to work with highlighting that our GO membranes can be produced on a high energy (PVDF) as well as a low energy (Nylon) substrate. The permeance behavior of the GO membrane in polar protic solvents (water, ethanol, methanol, IPA, 1- butanol) and a polar aprotic solvent (acetone), as well as non-polar solvents (Toluene and n-Hexane), were studied (Supplementary Section 10). In the molecular scale interlayer galleries, permeances will be governed by molecular scale solvent-membrane interactions as well as viscous forces. For polar solvents (Figure 5a), we realized that if the solvent-membrane interaction is scaled with dielectric constant (i.e. permeance$\times \frac{1}{\varepsilon}$), the permeance has a near-perfect inverse linear relationship with solvent viscosity as described by Hagen Poiseuille equation (i.e. permeance $\propto \frac{1}{\eta}$), on the other hand for the non-polar solvents, toluene and hexane, which has minimal interaction, permeance $\propto \frac{1}{\eta}$ as shown in inset of Figure 5a. Statistical analysis of fitting is discussed in Supplemental Section 10.

Comparison with commercial membrane: Finally the permeance performance of NF270, as a commercial nanofiltration membrane (Dow Chemical Company, USA), for the polar and non-polar solvent were investigated (Supplementary Section 10). Results revealed that permeance of NF270 for the solvents was much lower than the permeance of the GO membrane (Figure 5b). NF270 showed permeance of ~7-8 LMH/bar for water and methanol, 1.5±0.1 LMH/bar and

0.8±0.1 LMH/bar and 2.3±0.3 for ethanol and 1-butanol, and n-Hexane, respectively and did not permeate IPA as the charged NF 270 precludes the transport of non-polar molecule IPA. Most notably the permeance values are considerably smaller than our GO membranes. NF270 is unstable in acetone and toluene as the membrane dissolved, although this instability in acetone and toluene is likely from the polysulfone support. We, therefore, emphasize the versatility of GO membranes regarding solvent handling space compared to commercial polymeric membranes

Conclusions

Our investigations on the solvent transport properties of GO membranes show that the interactions (or the lack of) between the polar groups along the edges of the GO sheets and solvent plays a dominant role in the permeance and retention characteristics in polar mediums. The interlayer galleries of GO membrane are found to expand when in contact with the polar solvents and a power-law (0.48) dependence of experimental interlayer distance and dielectric constant indicates that electrostatics underpin this behavior. Despite having largest interlayer gallery distance in water, the trapped water molecules in the vicinity of charged carboxylate groups, enables a higher solute retention and lower permeance in a water medium compared to alcohols. For a wide variety of polar solvents we introduce a new scaling behavior, i.e. permeance $\propto \frac{1}{\varepsilon\eta}$, for predicting polar solvent flux through GO membrane. In consistence with our experiments, dwell time analysis using molecular dynamic simulations indicate that polar & charge-based interactions of the oxygenated functional groups with solvent molecules slows down transport rates. The stability and operability of GO membranes in a wide palette of polar protic, polar aprotic and non-polar solvents compared to a commercial nanofiltration membrane

along with the potential to be produced in large-areas using industrially scalable methods indicate selective separation applications of our membrane.

Methods:

Well-known modified Hummers method[51] was used to synthesize graphite oxide[51]. SP-1 grade 325 graphite powder purchased from Bay Carbon Inc., and sulfuric acid, potassium persulfate, phosphorus pentoxide and potassium permanganate supplied from Sigma-Aldrich. Exfoliated graphene oxide (GO) in DI water in a concentration of 1 mg/mL were prepared with aid of sonication (UP-100 Ultrasonic processor) of the graphite oxide, following by eliminating unexfoliated graphite oxide by centrifuge. Nematic liquid crystal of GO (30mg/mL) was synthesized by dehydration of the GO dispersion (1 mg/mL) with aid of superabsorbent polymer [5] (cross-linked polyacrylate copolymer based hydrogel beads, Demi Co., Ltd, China). The concentration of GO was determined by an Ocean Optics USB4000 UV-vis spectrometer, measuring the absorbance at 230 nm (using a quartz cuvette, Starna Cells Pty. Ltd, Australia) (More details in Supplementary Section 1).

In next stage, large-area GO membranes (13×14 cm^2), was fabricated on Polyvinylidene fluoride (PVDF) porous support (PVDF, pore size 0.2µm, MDI, India) by shear alignment of the nematic phase GO by a method reported elsewhere[5, 17, 18], with aid of conventional gravure printing machine (Labratester, Norbert Schläfli Machinery Company, Switzerland) (More details in Supplementary Section 2). The shear alignment membrane was further characterized by analysis, scanning electron microscopy (SEM) (More details in Supplementary Section 3), Fourier transforms infrared spectroscopy (FTIR) (More details in Supplementary Section 4), X-ray photoelectron spectroscopy (XPS) (More details in Supplementary Section 5) and X-ray

diffraction (XRD) (More details in Supplementary Section 6). The membrane was cut into the required size (47 mm diameter) for filtration tests after baking at 50 °C for 30 minutes[24] in a vacuum oven. The permselectivity behavior of the GO membrane in a different environment (aqueous and non–aqueous) was investigated by a dead-end filtration system (Sterlitech HP4750 High Pressure Stirred Cell) (More details in Supplementary Section 8).

AUTHOR INFORMATION

Corresponding Author

*Corresponding author E-mail: mainak.majumder@monash.edu

Author Contributions

AA designed and carried out experiments and analyzed the data. ES contributed in SEM and X-Ray diffraction measurements. CE contributed in XPS measurements, AA, SE, SM and MM co-wrote the article. BC contributed to the MD simulations with inputs from MM. All authors were involved in discussion & interpretation of data. MM oversaw the entire project.

ACKNOWLEDGMENT

Authors acknowledge funding from the Australian Research Council through an ARC Linkage (LP 140100959) grant and also partial support from University of Kentucky by NSF KY EPSCoR grant (Grant no: 1355438), NIH-NIEHS-SRC (Award number: P42ES007380). A. Akbari acknowledges the support of the Monash Centre for Atomically Thin Materials (MCATM).

FIGURES

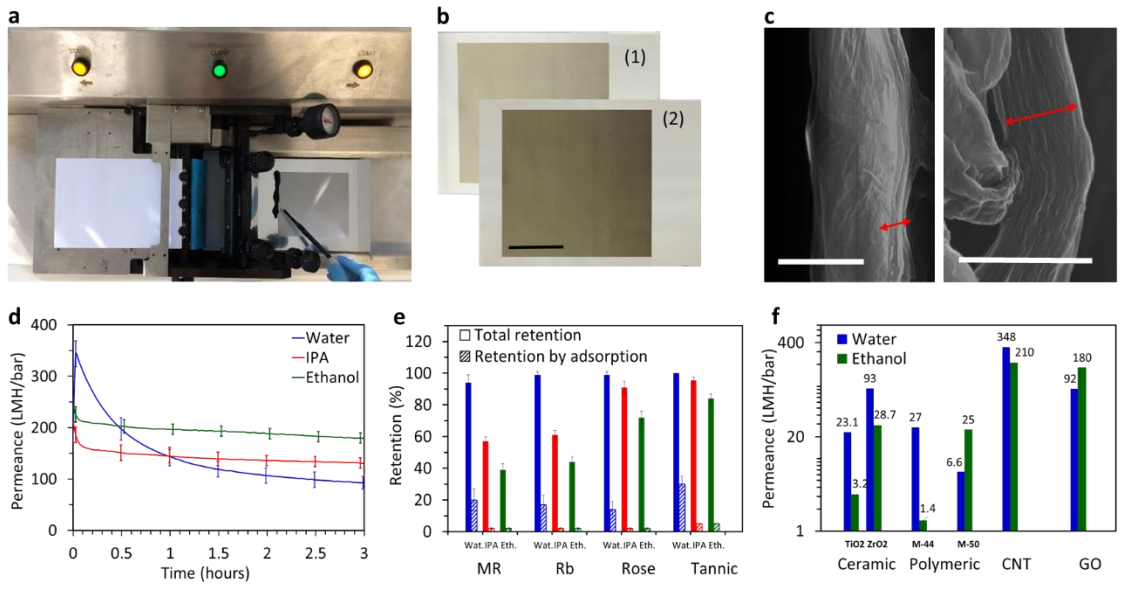

Figure 1. Permeance and retention behavior of the shear-aligned GO membrane. (a) Photograph of the gravure printing machine, used to fabricate GO membranes. **(b)** large-area GO membranes: (1) 100±20 nm thick on porous PVDF substrate, (2) 350±20 nm thickness on porous Nylon substrate. (Scale bar, 5 cm). **(c)** Cross-sectional SEM image of the PVDF supported GO membrane (left) and the Nylon supported GO membrane (right). The red arrows points the cross-sections. (Scale bars, 500 nm). (**d**) Plot demonstrates permeance of the PVDF-support GO membrane (under 0.25 bar pressure and at about 22 ℃) for water (blue), IPA (red), and ethanol (green). (**e**) The plain bars represent total retention of the PVDF-support GO membrane for the organic solutes (Methyl Red (MR), Rhodamine B (Rb), Rose Bengal (Rose), and Tannic Acid (Tannic), in different mediums (Water, IPA, and Ethanol), while striped bars show amount of the retention which is based on the adsorption mechanism (Wat. is water, IPA is isopropanol, and Eth. is ethanol) (under 0.25 bar pressure and at about 22 ℃). (**f**) Plot demonstrates a comparison between the PVDF-support GO membrane (from our project) with other nanofiltration membranes such as ceramic[37] (HITK275 and HITK2750, which are hydrophilic ceramic membranes consisting of a TiO_2 and ZrO_2 top layer, respectively), polymeric[31] (MPF-44 and MPF-50, which are hydrophilic and hydrophobic PDMS-based membranes, respectively) and carbon nanotube (CNT) membranes[32] in terms of membrane permeance and solvent polarity. M-44 and M50 are abbreviations of MPF-44 and MPF-50, respectively. Error bars: Standard deviations using at least five measurements from three different samples.

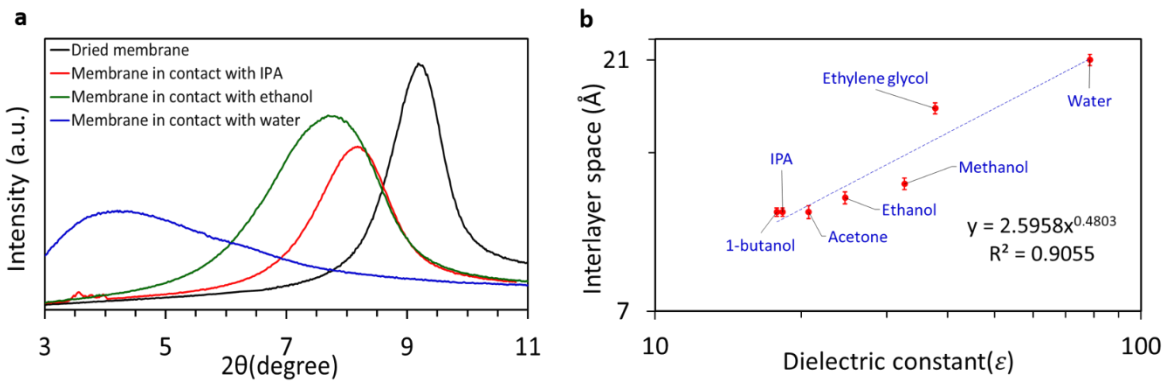

Figure 2. Effect of solvent on the interlayer space between GO sheets. (**a)** XRD of the GO membrane shows variance in interlayer space between GO sheets when the membrane is in contact with the different solvents (at about 22 ℃), (details in Table S1). (**b)** Plot demonstrates a logarithmic correlation between interlayer space of GO sheets and dielectric constant of selected polar solvents. Error bars: Standard deviations using at least three measurements from three different samples. Dashed line is a linear fit.

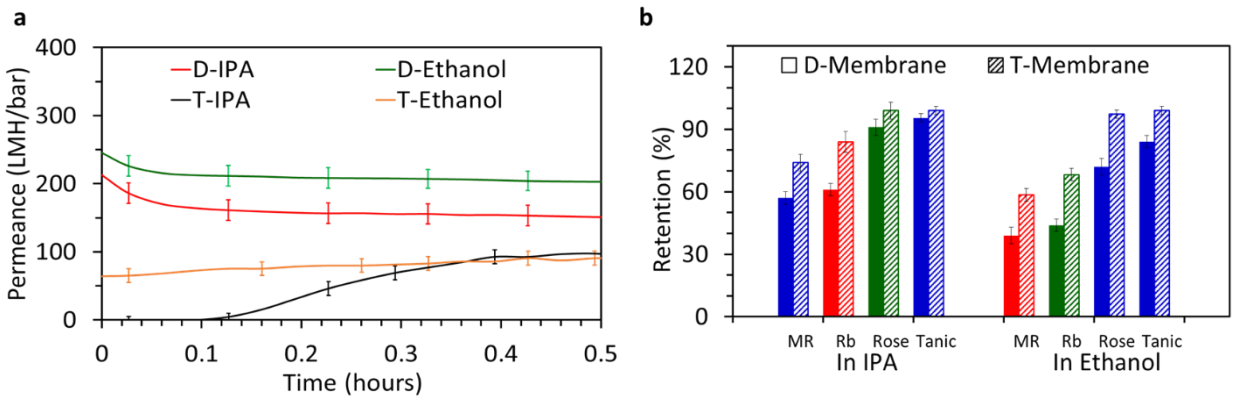

Figure 3. Transient permeance and retention behavior of the pre-treated GO membrane. **(a)** Plot demonstrates a comparison between the permeance of a GO membrane (100±20 nm thickness, under 0.25 bar pressure and at about 22 ℃) to the organic solvents, when the membrane is in a dried state (signed by the prefix of D-) and treated state (the dried GO membrane is pre-treated by soaking in water- signed by the prefix of T-). The permeance of the treated membrane to IPA and ethanol are less than the dried membrane, but the permeance increases with time, due to washing the GO nanochannels from water molecules. **(b)** The plot demonstrates how retention behavior of the GO membrane in the organic solvents improve when the membrane in pre-treated with water (under 0.25 bar pressure and about 22 ℃). The plain colors show retention of the dried membrane, while the striped show the retention for the pre-treated membrane. MR is Methyl Red, Rb is Rhodamine B, Rose is Rose Bengal, and Tannic is Tannic Acid. Error bars: Standard deviations using at least five measurements from three different samples.

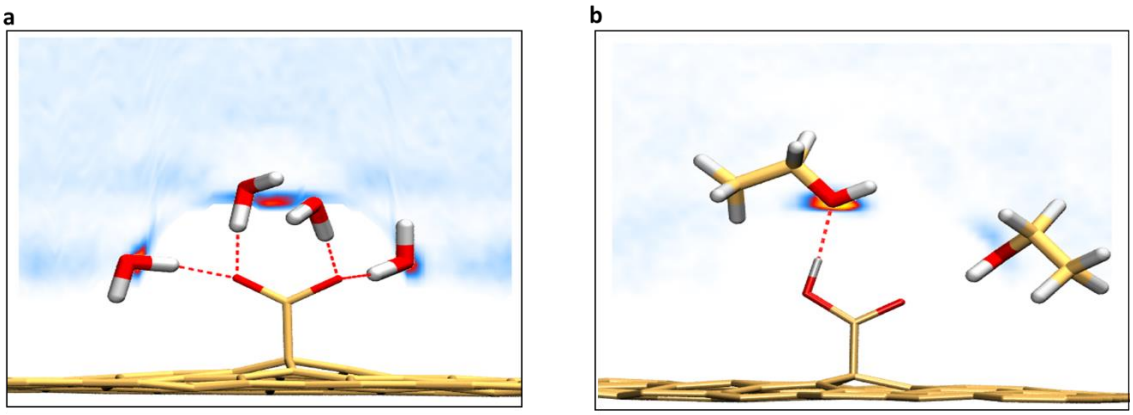

Figure 4. Simulation of interaction between GO surface and solvent. Snapshot of **a**) water neighbouring the carboxylate functional group and **b**) ethanol neighbouring the carboxyl group representing the interaction of solvent with the functional group in each case. The figures are superimposed on the average solvent oxygen density (white for low density, blue medium density and red/yellow for high density).

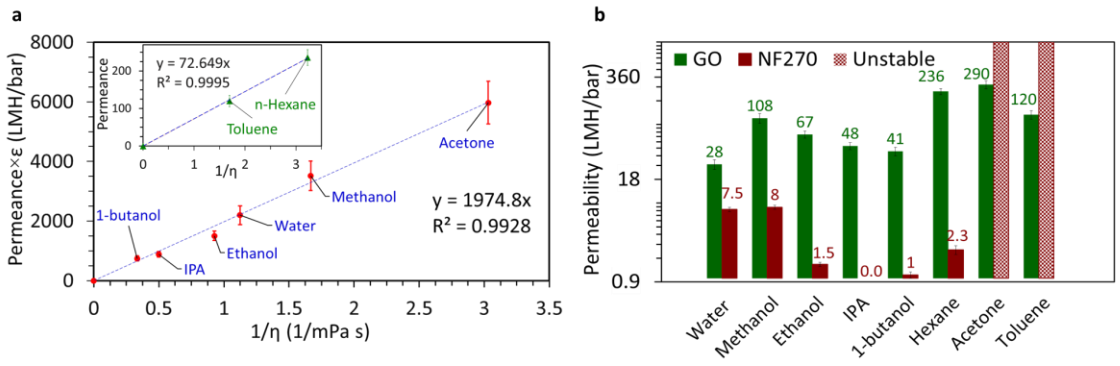

Figure 5. Permeance of GO membrane and commercial NF270 membrane. (a) Plot demonstrates an inverse linear relationship between the permeance of a GO membrane (Nylon-supported GO membrane with 350±20 nm thickness) and viscosity of permeating polar solvent, when the effect of polar-polar interactions between the membrane and solvents (quantified by dielectric constant) is scaled. Dashed line is a linear fit. Inset plot shows inverse linear relationship between the membrane permeance and viscosity of permeating non-polar solvents. **(b)** Plot demonstrates a comparison between the GO membrane (green color) and NF270 as a commercial nanofiltration membrane (dark brown color) in permeance for polar and non-polar solvents. The NF270 membrane was not stable in acetone and toluene and dissolved. (Tests carried out under 2 bar pressure under and at about 22 ℃). Error bars: Standard deviations using at least five measurements from three different samples.

TABLES.

Table 1. Dwell time simulation. Comparison of dwell time (ps) of the solvents near each functional group on a graphene surface. Entries most likely to be most influential on the transport rates on a GO surface are highlighted.

Solvent	**Water**	**Ethanol**	**IPA**
Pristine	10.5	33.1	44.8
Epoxy	76.3	133.3	125.4
Hydroxyl	130.1	336.5	427.1
Carboxyl	371.1	176.6	526.0
Carboxylate	1074.2	>=1912.5	>=2512.5

ASSOCIATED CONTENT:

The Supporting information is available. The supplementary Sections includes all details and condition of fabrication and characterization of the GO membrane.

REFERENCES

1. Joshi, R.; Carbone, P.; Wang, F.-C.; Kravets, V. G.; Su, Y.; Grigorieva, I. V.; Wu, H.; Geim, A. K.; Nair, R. R., Precise and ultrafast molecular sieving through graphene oxide membranes. *Science* **2014**, 343, 752-754.
2. Akbari, A.; Sheath, P.; Martin, S. T.; Shinde, D. B.; Shaibani, M.; Banerjee, P. C.; Tkacz, R.; Bhattacharyya, D.; Majumder, M., Large-area graphene-based nanofiltration membranes by shear alignment of discotic nematic liquid crystals of graphene oxide. *Nat Commun* **2016**, 7.
3. Kim, H. W.; Yoon, H. W.; Yoon, S.-M.; Yoo, B. M.; Ahn, B. K.; Cho, Y. H.; Shin, H. J.; Yang, H.; Paik, U.; Kwon, S., Selective gas transport through few-layered graphene and graphene oxide membranes. *Science* **2013**, 342, 91-95.
4. Gao, W.; Singh, N.; Song, L.; Liu, Z.; Reddy, A. L. M.; Ci, L.; Vajtai, R.; Zhang, Q.; Wei, B.; Ajayan, P. M., Direct laser writing of micro-supercapacitors on hydrated graphite oxide films. *Nature Nanotechnology* **2011**, 6, 496-500.
5. Shaibani, M.; Akbari, A.; Sheath, P.; Easton, C. D.; Banerjee, P. C.; Konstas, K.; Fakhfouri, A.; Barghamadi, M.; Musameh, M. M.; Best, A. S., Suppressed Polysulfide Crossover in Li-S Batteries Through a High-Flux Graphene Oxide Membrane Supported on Sulfur Cathode. *ACS nano* **2016**, 10, 7768–7779
6. Yoon, H. J.; Kim, T. H.; Zhang, Z.; Azizi, E.; Pham, T. M.; Paoletti, C.; Lin, J.; Ramnath, N.; Wicha, M. S.; Hayes, D. F., Sensitive capture of circulating tumour cells by functionalized graphene oxide nanosheets. *Nature nanotechnology* **2013**, 8, 735-741.
7. Kovtyukhova, N. I.; Ollivier, P. J.; Martin, B. R.; Mallouk, T. E.; Chizhik, S. A.; Buzaneva, E. V.; Gorchinskiy, A. D., Layer-by-layer assembly of ultrathin composite films from micron-sized graphite oxide sheets and polycations. *Chemistry of Materials* **1999**, 11, 771-778.
8. Dreyer, D. R.; Park, S.; Bielawski, C. W.; Ruoff, R. S., The chemistry of graphene oxide. *Chemical Society Reviews* **2010**, 39, 228-240.
9. Geim, A. K.; Nair, R. R., Tunable sieving of ions using graphene oxide membranes. **2017**, 12, 546–550.
10. Nair, R.; Wu, H.; Jayaram, P.; Grigorieva, I.; Geim, A., Unimpeded permeation of water through helium-leak–tight graphene-based membranes. *Science* **2012**, 335, 442-444.
11. Li, H.; Song, Z.; Zhang, X.; Huang, Y.; Li, S.; Mao, Y.; Ploehn, H. J.; Bao, Y.; Yu, M., Ultrathin, Molecular-Sieving Graphene Oxide Membranes for Selective Hydrogen Separation. *Science* **2013**, 342, 95-98.
12. Huang, K.; Liu, G.; Lou, Y.; Dong, Z.; Shen, J.; Jin, W., A graphene oxide membrane with highly selective molecular separation of aqueous organic solution. *Angewandte Chemie International Edition* **2014**, 53, 6929-6932.
13. Gao, Y.; Hu, M.; Mi, B., Membrane surface modification with TiO 2–graphene oxide for enhanced photocatalytic performance. *Journal of Membrane Science* **2014**, 455, 349-356.

14. Rashidi, F.; Kevlich, N. S.; Sinquefield, S.; Shofner, M. L.; Nair, S., Graphene Oxide Membranes in Extreme Operating Environments: Concentration of Kraft Black Liquor by Lignin Retention. *ACS Sustainable Chemistry & Engineering* **2016**, 5, 1002–1009.
15. Dikin, D. A.; Stankovich, S.; Zimney, E. J.; Piner, R. D.; Dommett, G. H.; Evmenenko, G.; Nguyen, S. T.; Ruoff, R. S., Preparation and characterization of graphene oxide paper. *Nature* **2007**, 448, 457-460.
16. Hu, M.; Mi, B., Layer-by-layer assembly of graphene oxide membranes via electrostatic interaction. *Journal of Membrane Science* **2014**, 469, 80-87.
17. Coskun, M. B.; Akbari, A.; Lai, D. T.; Neild, A.; Majumder, M.; Alan, T., Ultrasensitive Strain Sensor Produced by Direct Patterning of Liquid Crystals of Graphene Oxide on a Flexible Substrate. *ACS applied materials & interfaces* **2016**, 8, 22501-22505.
18. Martin, S. T.; Akbari, A.; Banerjee, P. C.; Neild, A.; Majumder, M., The inside-out supercapacitor: induced charge storage in reduced graphene oxide. *Physical Chemistry Chemical Physics* **2016**, 18, 32185-32191.
19. Israelachvili, J. N., *Intermolecular and surface forces*. Academic press: 2011.
20. Cote, L. J.; Kim, J.; Tung, V. C.; Luo, J.; Kim, F.; Huang, J., Graphene oxide as surfactant sheets. *Pure and Applied Chemistry* **2010**, 83, 95-110.
21. Kim, J.; Cote, L. J.; Kim, F.; Yuan, W.; Shull, K. R.; Huang, J., Graphene oxide sheets at interfaces. *Journal of the American Chemical Society* **2010**, 132, 8180-8186.
22. Jalili, R.; Aboutalebi, S. H.; Esrafilzadeh, D.; Konstantinov, K.; Moulton, S. E.; Razal, J. M.; Wallace, G. G., Organic solvent-based graphene oxide liquid crystals: a facile route toward the next generation of self-assembled layer-by-layer multifunctional 3D architectures. *Acs Nano* **2013**, 7, 3981-3990.
23. Huang, L.; Li, Y.; Zhou, Q.; Yuan, W.; Shi, G., Graphene oxide membranes with tunable semipermeability in organic solvents. *Advanced Materials* **2015**, 27, 3797-3802.
24. Aher, A.; Cai, Y.; Majumder, M.; Bhattacharyya, D., Synthesis of graphene oxide membranes and their behavior in water and isopropanol. *Carbon* **2017**, 116, 145-153.
25. Huang, L.; Chen, J.; Gao, T.; Zhang, M.; Li, Y.; Dai, L.; Qu, L.; Shi, G., Reduced graphene oxide membranes for ultrafast organic solvent nanofiltration. *Advanced Materials* **2016**, 28, 8669-8674.
26. Boukhvalov, D. W.; Katsnelson, M. I.; Son, Y. W., Origin of anomalous water permeation through graphene oxide membrane. *Nano letters* **2013**, 13, 3930-5.
27. Dai, H.; Xu, Z.; Yang, X., Water Permeation and Ion Rejection in Layer-by-Layer Stacked Graphene Oxide Nanochannels: A Molecular Dynamics Simulation. *The Journal of Physical Chemistry C* **2016**, 120, 22585-22596.
28. Cerveny, S.; Barroso-Bujans, F.; Alegria, A.; Colmenero, J., Dynamics of water intercalated in graphite oxide. *The Journal of Physical Chemistry C* **2010**, 114, 2604-2612.
29. Li, J.; Gong, X.; Lu, H.; Li, D.; Fang, H.; Zhou, R., Electrostatic gating of a nanometer water channel. *Proceedings of the National Academy of Sciences* **2007**, 104, 3687-3692.
30. Yang, X.; Livingston, A.; Dos Santos, L. F., Experimental observations of nanofiltration with organic solvents. *Journal of Membrane Science* **2001**, 190, 45-55.
31. Zhao, Y.; Yuan, Q., A comparison of nanofiltration with aqueous and organic solvents. *Journal of membrane science* **2006**, 279, 453-458.
32. Majumder, M.; Chopra, N.; Andrews, R.; Hinds, B. J., Nanoscale hydrodynamics: enhanced flow in carbon nanotubes. *Nature* **2005**, 438, 44-44.

33. Wei, N.; Peng, X.; Xu, Z., Breakdown of fast water transport in graphene oxides. *Physical Review E* **2014**, 89, 012113.
34. Wei, N.; Peng, X.; Xu, Z., Understanding water permeation in graphene oxide membranes. *ACS applied materials & interfaces* **2014**, 6, 5877-5883.
35. Zheng, J.; Lennon, E. M.; Tsao, H.-K.; Sheng, Y.-J.; Jiang, S., Transport of a liquid water and methanol mixture through carbon nanotubes under a chemical potential gradient. *The Journal of chemical physics* **2005**, 122, 214702.
36. Van der Bruggen, B.; Geens, J.; Vandecasteele, C., Fluxes and rejections for nanofiltration with solvent stable polymeric membranes in water, ethanol and n-hexane. *Chemical engineering science* **2002**, 57, 2511-2518.
37. Darvishmanesh, S.; Buekenhoudt, A.; Degrève, J.; Van der Bruggen, B., Coupled series–parallel resistance model for transport of solvent through inorganic nanofiltration membranes. *Separation and Purification Technology* **2009**, 70, 46-52.
38. Moazzami Gudarzi, M., Colloidal Stability of Graphene Oxide: Aggregation in Two Dimensions. *Langmuir* **2016**, 32, 5058–5068.
39. Gravelle, S.; Yoshida, H.; Joly, L.; Ybert, C.; Bocquet, L., Carbon membranes for efficient water-ethanol separation. *The Journal of Chemical Physics* **2016**, 145, 124708.
40. DeRuiter, J., Carboxylic Acid Structure and Chemistry: Part 1. *Principles of drug action I. Auburn University, Alabama* **2005**, 1-11.
41. DeRuiter, J., Carboxylic Acid Structure and Chemistry: Part 2. *Principles of Drug Action 1. Aubum University, Alabama* **2005**, 1-10.
42. Anslyn, E. V.; Dougherty, D. A., *Modern physical organic chemistry*. University Science Books: 2006.
43. Geens, J.; Boussu, K.; Vandecasteele, C.; Van der Bruggen, B., Modelling of solute transport in non-aqueous nanofiltration. *Journal of Membrane Science* **2006**, 281, 139-148.
44. Han, Y.; Xu, Z.; Gao, C., Ultrathin Graphene Nanofiltration Membrane for Water Purification. *Advanced Functional Materials* **2013**, 23, 3693-3700.
45. Smallwood, I., *Handbook of organic solvent properties*. Butterworth-Heinemann: 2012.
46. Israelachvili, J. N., *Intermolecular and surface forces: revised third edition*. Academic press: 2011.
47. Parsegian, V. A., *Van der Waals forces: a handbook for biologists, chemists, engineers, and physicists*. Cambridge University Press: 2005.
48. Zheng, S.; Tu, Q.; Urban, J. J.; Li, S.; Mi, B., Swelling of Graphene Oxide Membranes in Aqueous Solution: Characterization of Interlayer Spacing and Insight into Water Transport Mechanisms. *ACS Nano* **2017**, 11, 6440-6450.
49. Phan, A.; Cole, D. R.; Weiß, R. G.; Dzubiella, J.; Striolo, A., Confined Water Determines Transport Properties of Guest Molecules in Narrow Pores. *ACS nano* **2016**, 10, 7646-7656.
50. Carson, S.; Wilson, J.; Aksimentiev, A.; Wanunu, M., Smooth DNA transport through a narrowed pore geometry. *Biophysical journal* **2014**, 107, 2381-2393.
51. Hummers Jr, W. S.; Offeman, R. E., Preparation of graphitic oxide. *Journal of the American Chemical Society* **1958**, 80, 1339-1339.

Table of contents graphic: